

Topologically entangled Rashba-split bands on the grey arsenic surface

Peng Zhang^{1,2,*}, J.-Z. Ma^{2,*}, Yukiaki Ishida^{1,*}, Q.-N. Xu², B.-Q. Lv², Koichiro Yaji¹, L.-X. Zhao², G.-F. Chen^{2,3}, H.-M. Weng^{2,3}, X. Dai^{2,3}, Z. Fang^{2,3}, X.-Q. Chen⁴, L. Fu⁵, T. Qian^{2,3,†}, H. Ding^{2,3,†}, & Shik Shin^{1,†}

¹*ISSP, University of Tokyo, Kashiwa, Chiba 277-8581, Japan*

²*Beijing National Laboratory for Condensed Matter Physics, and Institute of Physics, Chinese Academy of Sciences, Beijing 100190, China*

³*Collaborative Innovation Center of Quantum Matter, Beijing, China*

⁴*Shenyang National Laboratory for Materials Science, Institute of Metal Research, Chinese Academy of Science, Shenyang 110016, China*

⁵*Department of Physics, Massachusetts Institute of Technology, Cambridge, Massachusetts 02139, USA*

** These authors contributed equally to this work*

Rashba-split states are discovered on the surfaces of many semi-infinite single crystals. They are generally explained based on the Rashba theory, considering spin-orbit coupling (SOC) and inversion symmetry breaking on the surface. Here we investigate the electronic structures of grey arsenic by means of angle-resolved photoemission spectroscopy (ARPES). We discover a pair of Rashba-split surface bands occurring on As(111) surface. By utilizing pump-and-probe ARPES, the pair is shown to be topologically entangled between bulk va-

lence and conduction bands. Our results provide compelling evidence that the spin-split bands found on As(111) are guaranteed by the topology of the band structures that is beyond the genuine Rashba band splitting. Our findings establish a new paradigm in the understanding of the spin-split surface states.

Single crystals formed by Group V elements have plenty of interesting properties. Black phosphor, arsenic, antimony and bismuth are well-known semimetals. Black phosphor is famous for the tunable Dirac-like bulk band, which provides great flexibility in design of electronic devices¹. Sb and Bi both possess spin-split surface states²⁻⁸, and their alloy is the first discovered 3D topological insulator⁹. However, the electronic structure of arsenic is rarely investigated. Here we present the first band structure measurement and show that gray arsenic has a topologically entangled Rashba-split surface state.

Arsenic has three types of elemental crystals: grey, yellow, and black arsenic. In this work, we systematically investigate the electronic structure of grey arsenic, which has a rhombohedral unit cell with space group of R3m (No. 166). As shown in Fig. 1a, the crystal can be regarded as a stack of As bilayer along the [111] direction. The As atoms within the bilayer form a buckled honeycomb lattice. The bulk BZ as well as its projected (111) surface BZ is shown in Fig. 1b. The projection of the bulk bands on the (111) surface in Fig. 1c provides an easy view of the overall bulk band structure, which shows a semimetal feature, i.e., there exists a direct energy gap between the conduction and valence bands at every momentum point in the whole BZ while no indirect energy gap. In addition to the calculated bulk band structure, we find a pair of parabolic

bands occurring around the surface Brillouin-zone center $\bar{\Gamma}$, which are split along both $\bar{\Gamma} - \bar{M}$ and $\bar{\Gamma} - \bar{K}$ directions but degenerate at the time-reversal invariant momentum (TRIM) $\bar{\Gamma}$ (Fig. 1e - f), and forms two almost isotropic concentric FSs enclosing the $\bar{\Gamma}$ point (Fig. 1d). The pair mimics the spin-split surface states induced by the Rashba-type interaction. The surface localized nature of these two bands is further confirmed experimentally by investigating the band dispersions along k_z . By mapping the Fermi surface in k_y - k_z space, we find that the Fermi momentum k_F is localized at $k_y = \pm 0.065 \text{ \AA}^{-1}$ throughout k_z (Blue arrow in Fig. S1). Additionally, the bands with large k_z dispersion shows quite small spin-polarization, while the two parabolic bands around $\bar{\Gamma}$ show strong spin polarization, further confirming their bulk and surface nature (Fig. S2).

The spin polarization of the two surface bands are investigated by using spin-resolved ARPES (SARPES)¹⁰, as shown in Fig. 1f. Here, we plotted the intensity difference between spin up and spin down along x direction of the photoelectrons detected by the VLEED detector. The spin polarization is about 40~60 % along the $\bar{\Gamma} - \bar{K}$ direction. In contrast, no significant spin polarizations are observed along the y and z directions (see Supplementary Section II). Thus, we confirmed the spin-split surface state observed on As (111) is Rashba-split state, which is well-known on the surfaces of noble metals^{11,12}. In the nearly-free-electron (NFE) model, the band dispersions of Rashba-split states follow $H(k) = E_0 + \frac{\hbar k^2}{2m^*} \pm \alpha k$, where α is the Rashba parameter, characterizing the strength of the Rashba effect¹³. Fig. 1h shows that the band dispersions of As (111) surface state can be well fit to the NFE model. The fitting gives a Rashba-parameter of 1.0 eV \AA , and an effective electron mass of $0.07 m_e$.

More surprisingly, here we show that the spin-split surface bands discovered on As(111) are topologically non-trivial in the sense that they cannot be described by the simple surface Rashba splitting. Fig.2 shows the band dispersions revealed into the unoccupied side by using the pump-and-probe method: When impinged by an intense femtosecond pump pulse, electrons are redistributed into the unoccupied side, so that the bands therein can be observed¹⁴. The excitation/decay process of the states above E_F in the $\bar{\Gamma} - \bar{K}$ direction with various pump-probe delay times is displayed in Fig. 2b. Although the NFE model fits well to the occupied surface states around $\bar{\Gamma}$, we clearly reveal an obvious deviation in the unoccupied state in both $\bar{\Gamma} - \bar{M}$ and $\bar{\Gamma} - \bar{K}$ directions. In the $\bar{\Gamma} - \bar{K}$ direction, one of the pair extends into the conduction band, while the other turns back and merges into the valence band. Thus, the spin-split pair of the surface bands is topologically entangled, or each of the pair disperses from the valence to conduction band to form an unavoidable crossing. Along the $\bar{\Gamma} - \bar{M}$ direction, the topological connection between the surface and bulk states is not directly determined from the experimental data, but confirmed by first principle calculations shown below. Fig. 2c summarizes the band structure below and above E_F and clearly shows the entanglement of the surface and bulk bands.

We perform first-principle calculations to illuminate the topological properties of the band structure. Without SOC, there is a band crossing slightly above E_F along T-W (Fig. 3a), and the band crossings in the whole BZ form a Dirac nodal line, as shown in Fig.S4, Supplementary Section III. We denote the band crossing point along T-W as S (Fig. 3b). When the SOC is turned on, an energy gap is opened at the S point, leading to a direct energy gap in the whole BZ. Since this material has inversion symmetry, we can get its Z_2 indices from the parity product

Table 1: Parities of gray As

TRIMs	Parities of occupied bands	Product
1 Γ	+ - + + +	-
3 L	+ - - + +	+
3 X	- + + - -	-
1 T	- + - - +	-
$Z_2(1;111)$		

at the eight TRIMs, which are shown in Table 1. The Z_2 invariant is (1;111), indicating that the gray As has a strong topological surface state, which can be regarded as evolved from the topological surface state hosted by the 3D Dirac nodal-line semimetal state in the absence of SOC. In Fig. 3d, we present the slab calculations of surface and bulk band structures, which reproduce well the experimental results. Around $\bar{\Gamma}$, the surface bands follow the NFE behavior well. As the surface state bands approach the S point, they connect to the conduction and valence bulk states, respectively. The lower branch of the surface state bands bends downwards as it merges into the valence bulk states. This leads to a flower-like surface state FS enclosing the projected FS continuum of the valence bulk states, as schematically shown in Fig. 3e. This surface state FS with a six-fold symmetry is confirmed by our FS mapping measurement (Fig. 3f). There are three surface state FSs enclosing the TRIM $\bar{\Gamma}$ point, which supports a nonzero Berry's phase. This is different from the conventional Rashba-split states, in which two concentric spin-polarized FSs enclose $\bar{\Gamma}$.

The conventional Rashba-split bands originate from the SOC and effective electric field that describes the inversion symmetry breaking on the surface^{13,15–17}, in which the band splitting itself has no connection with the band topology. While in the As case, the spin-splitting near $\bar{\Gamma}$ is dominated by the Rashba effect, but the surface state is topologically entangled and thus its existence is guaranteed by the bulk band topology. In this sense we classify this new type of surface state in As to be topological Rashba-split state. There are emerging proposals for reexamining the topological nature of surface states on elementary single crystals. For example, it is recently predicted that beryllium is a Dirac nodal line semimetal and the surface state is topological nontrivial¹⁸. There is also a proposal to explain the Rashba-split surface states on Au as topologically nontrivial¹⁹. However, experimental confirmations of such proposals are difficult, either because of the small energy scale in beryllium or band connections far above E_F in Au. Instead, our results on arsenic (111) surface provides a clear and convincing observation of the topological entanglement of the NFE Rashba-split states, and establish a new paradigm in understanding surface states on simple materials^{18–21}.

Method Single crystals of grey arsenic were grown from the vapor. ARPES experiment was carried out in ISSP, Tokyo University with 6eV and 7eV lasers and at the Dreamline beamline of the Shanghai Synchrotron Radiation Facility (SSRF). The vacuum is better than $<5 \times 10^{-11}$ Torr for all the ARPES measurements. The ARPES system at SSRF is equipped with Scienta D80 analyzer, with a resolution of about 15meV.

TARPES measurements were carried out using a hemispherical Scienta-Omicron R4000 an-

alyzer and a mode-locked Ti:sapphire laser system delivering 1.48-eV pump and 5.92-eV probe pulses at the repetition rate of 250 kHz¹⁴. The time and energy resolutions were 280 fs and 15 meV, respectively. The spot diameters of the pump and probe beams at the sample were 250 μm and 85 μm , respectively.

Laser-SARPES measurements were carried out using a custom-made ScientaOmicron DA30-L attached with twin VLEED spin detectors and a VUV laser system delivering 6.994-eV photons¹⁰. The energy resolution and spot diameter were set to 15 \sim 20 meV and \sim 100 μm , respectively.

The band structure was calculated by the first-principles calculation program package the Vienna ab initio simulation package (VASP). The exchange-correlation potential used is the generalized gradient approximation (GGA) of Perdew-Burke-Ernzerhof(PBE) type. The cut-off energy for plane wave expansion is 400 eV and the k-point grid in the self-consistent process is $8 \times 8 \times 8$ for 3D bulk calculation. The package wannier90 is used to obtain Maximally-Localized Wannier Functions (MLWFs) of p orbitals of As. The Green's function method based on tight-binding model with MLWFs as bases is used to get the edge state.

1. Kim, J. et al. Observation of tunable band gap and anisotropic Dirac semimetal state in black phosphorus. Science **349**, 723 (2015).
2. Thomas, J., Jezequel, G. & Pollini, I. Photoemission study of the bulk and surface electronic structure of Bi(111). J. Phys.: Condens. Matter **11**, 9571 (1999).
3. Tanaka, A. et al. Bulk and surface electronic structures of the semimetal Bi studied by angle-

- resolved photoemission spectroscopy. Phys. Rev. B **59**, 1786 (1999).
4. Ast, C. R. & Höchst, H. Fermi Surface of Bi(111) Measured by Photoemission Spectroscopy. Phys. Rev. Lett. **87**, 177602 (2001).
 5. Koroteev, Y. M. et al. Strong Spin-Orbit Splitting on Bi Surfaces. Phys. Rev. Lett. **93**, 046403 (2004).
 6. Sugawara, K. et al. Fermi Surface and Anisotropic Spin-Orbit Coupling of Sb(111) Studied by Angle-Resolved Photoemission Spectroscopy. Phys. Rev. Lett. **96**, 046411 (2006).
 7. Hsieh, D. et al. Observation of Unconventional Quantum Spin Textures in Topological Insulators. Science **323**, 919 (2009).
 8. Bian, G., Miller, T. & Chiang, T.-C. Passage from Spin-Polarized Surface States to Unpolarized Quantum Well States in Topologically Nontrivial Sb Films. Phys. Rev. Lett. **107**, 036802 (2011).
 9. Hsieh, D. et al. A topological Dirac insulator in a quantum spin Hall phase. Nature **452**, 970 (2008).
 10. Yaji, K. et al. High-resolution three-dimensional spin- and angle-resolved photoelectron spectrometer using vacuum ultraviolet laser light. Rev. Sci. Instrum. **87**, 053111 (2016).
 11. LaShell, S., McDougall, B. A. & Jensen, E. Spin Splitting of an Au(111) Surface State Band Observed with Angle Resolved Photoelectron Spectroscopy. Phys. Rev. Lett. **77**, 3419 (1996).

12. Tamai, A. et al. Spin-orbit splitting of the Shockley surface state on Cu(111). Phys. Rev. B **87**, 075113 (2013).
13. Bychkov, Y. A. & Rashba, E. I. Properties of a 2D electron gas with lifted spectral degeneracy. JETP Lett. **39**, 78 (1984).
14. Ishida, Y. et al. Time-resolved photoemission apparatus achieving sub-20-meV energy resolution and high stability. Rev. Sci. Instrum. **85**, 123904 (2014).
15. Petersen, L. & Hedegård, P. A simple tight-binding model of spin-orbit splitting of sp-derived surface states. Surf. Sci. **459**, 49 (2000).
16. Nagano, M., Kodama, A., Shishidou, T. & Oguchi, T. A first-principles study on the Rashba effect in surface systems. J. Phys.: Condens. Matter **21**, 064239 (2009).
17. Krasovskii, E. E. Microscopic origin of the relativistic splitting of surface states. Phys. Rev. B **90**, 115434 (2014).
18. Li, R. et al. Dirac node lines in pure alkali earth metals (2016). URL <http://arxiv.org/abs/1603.03974v2>. 1603.03974v2.
19. Yan, B. et al. Topological states on the gold surface. Nat. Commun. **6**, 10167 (2015).
20. Ohtsubo, Y. et al. Non-trivial surface-band dispersion on Bi(111). New J. Phys. **15**, 033041 (2013).

21. Ito, S. et al. Evolution in electronic structures of quasi-three-dimensional Bi films: evidence for nontrivial topology of Bi (2016). URL <http://arxiv.org/abs/1605.03531v1>.
[1605.03531v1](http://arxiv.org/abs/1605.03531v1).

Acknowledgements We acknowledge T. Kondo, K. Kuroda, Z. J. Wang and X. X. Wu for useful discussions. This work was supported by Photon and Quantum Basic Research Coordinated Development Program from MEXT, JSPS (KAKENHI Grants No. 25220707, 26800165, and Grant-in-Aid for Young Scientists (B), Grant No. 15K17675), the Ministry of Science and Technology of China (Nos. 2013CB921700 and 2015CB921300), the National Natural Science Foundation of China (Nos. 11234014, 11274359, 11422428 and 11474340), the Chinese Academy of Sciences (No. XDB07000000), and MOST project under the contract number 2016YFA0300604. Part of the calculations were performed on TianHe-1(A), the National Supercomputer Center in Tianjin, China.

Competing Interests The authors declare that they have no competing financial interests.

Correspondence Correspondence and request for materials should be addressed to T.Q., H.D. or S.S. (emails: tqian@iphy.ac.cn, dingh@iphy.ac.cn, shin@issp.u-tokyo.ac.jp)

Author contributions P.Z., J.Z.M., Y.I. and B.Q.L. did the ARPES measurements with assistance from K.Y., L.X.Z. and G.F.C. synthesized the samples. Q.N.X., H.M.W., X.D. and F.Z. did the LDA calculation. X.Q.C. and L.F. provided theoretical explanations and improved the manuscript. P.Z. analyzed the data. P.Z., Y.I. and T.Q. wrote the manuscript. T. Q., H.D. and S.S. supervised the project. All authors discussed the paper.

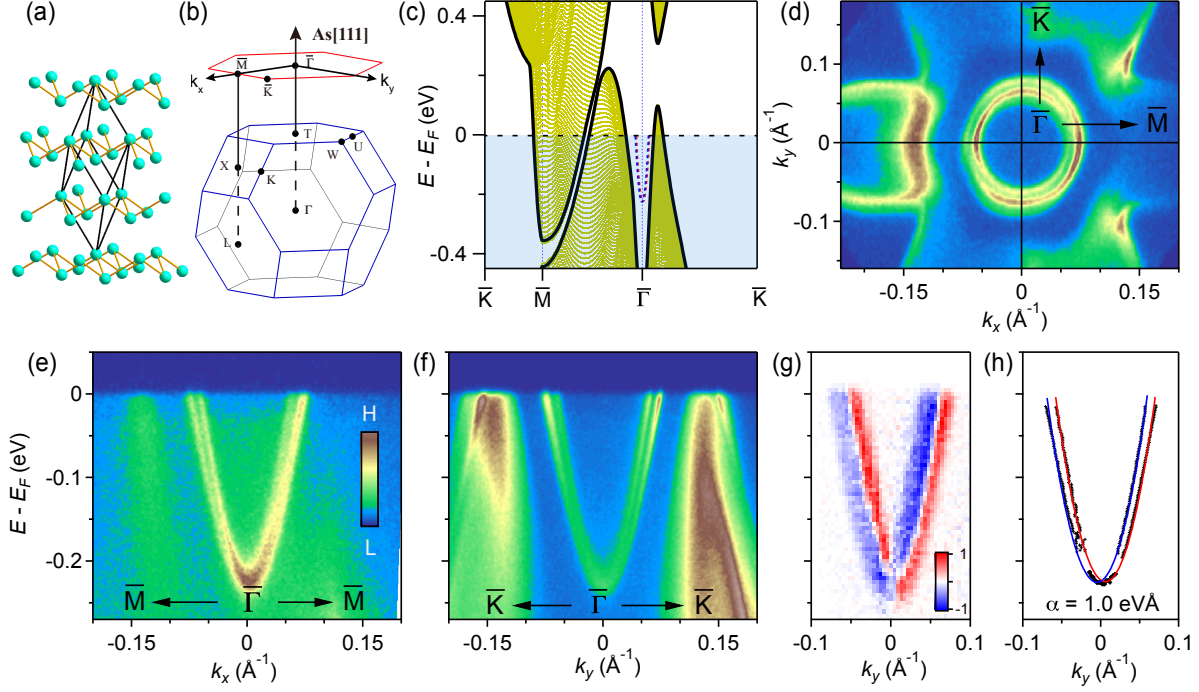


Figure 1: (a) Crystal structure of grey arsenic and (b) its Brillouin zones of bulk and (111) surface. (c) Projection of bulk bands onto As(111) surface. The two dashed curves are the fitting result in (h). (d) FS mapping at 10K with 7eV laser. (e - f) High symmetry cut along $\bar{\Gamma}\bar{M}$ and $\bar{\Gamma}\bar{K}$ directions taken at 10K. (g) Spin-polarized high symmetry cut along $\bar{\Gamma}\bar{K}$ direction taken at 10K. (h) Parabolic fittings of the two bands. The fittings use a combination of EDC (bottom part) and MDC peaks.

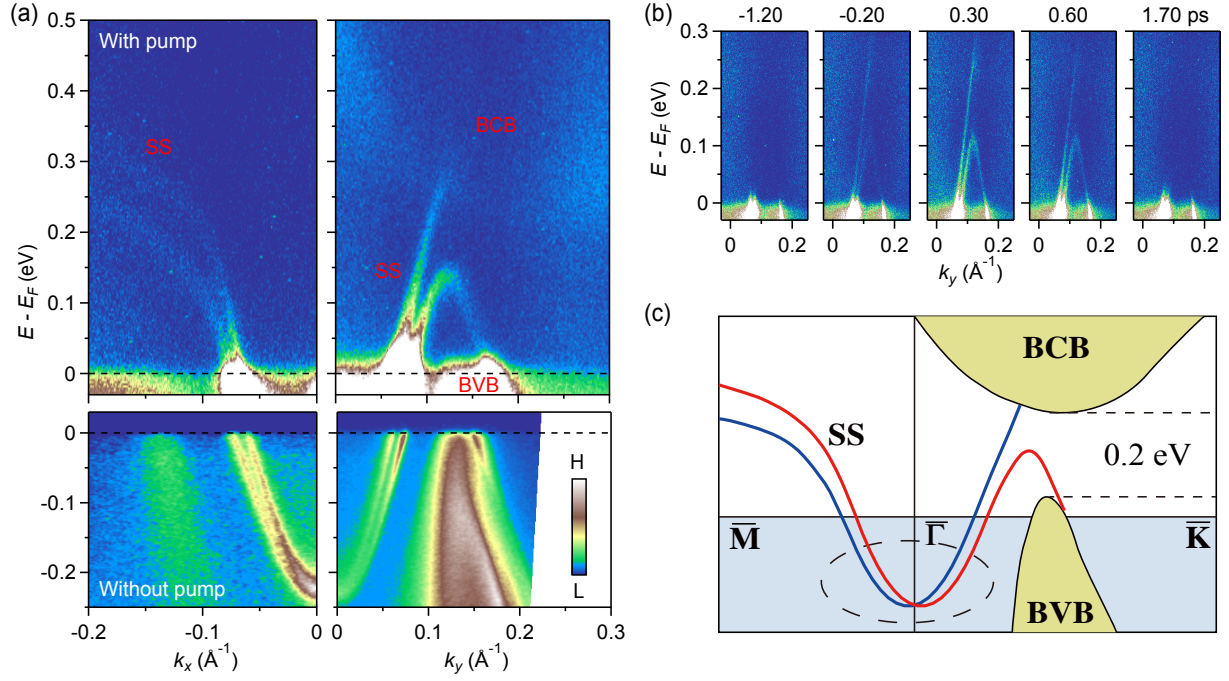


Figure 2: (a) Band structure below and above E_F taken at 10 K. Top-left and bottom-left panels: Band structure along $\bar{\Gamma}\bar{M}$ with and without pump photons. Top-right and bottom right panels: band structure along $\bar{\Gamma}\bar{K}$ with and without pump photons. (b) Excitation and decay of electrons above E_F with various pump-probe delays. (c) Cartoon on the topology of the experimental band structure. Red and blue lines indicate the surface bands with different spin orientations.

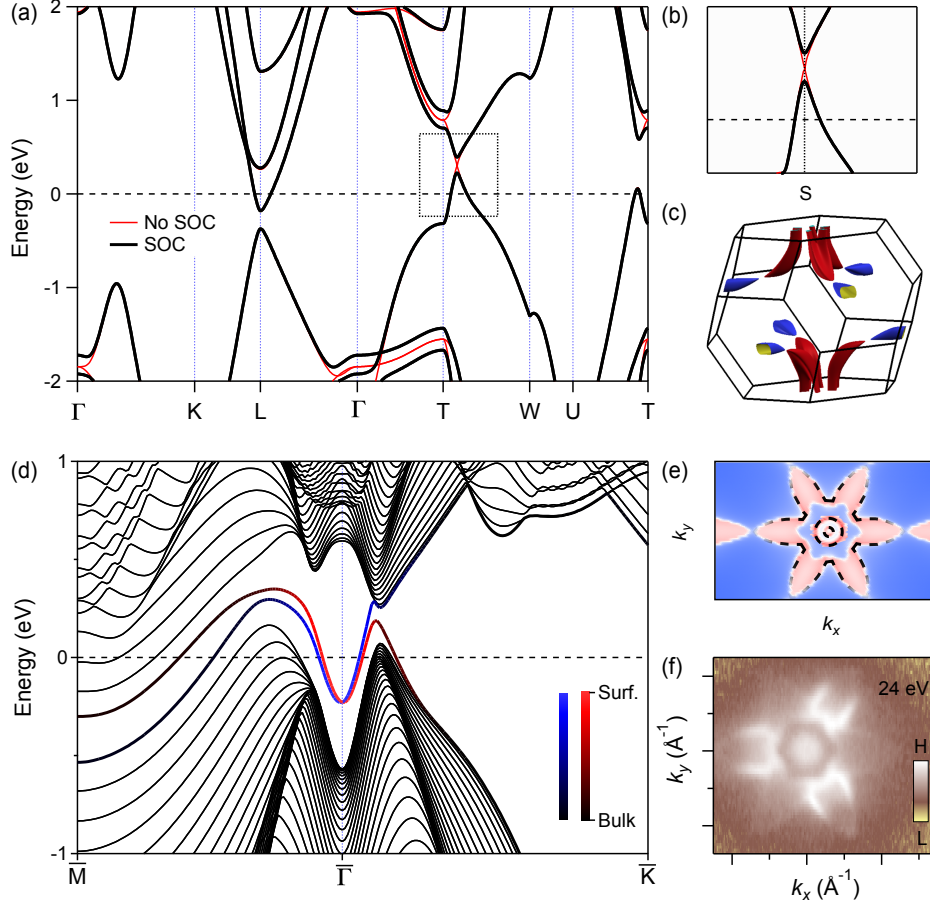


Figure 3: (a) Bulk band structure of gray As from LDA calculation. (b) Zoom-in display of the dashed box in (a). (c) 3D FS from LDA calculation. (d) Surface and bulk bands along high symmetry lines $\bar{\Gamma}\bar{K}$ and $\bar{\Gamma}\bar{M}$ from slab calculation. The surface components are shown with blue and red lines, while bulk components are shown with black lines. (e) FS projected to As(111) surface from tight-binding calculation. The dashed black lines indicate the surface state FSs. (f) FS measured at 24 eV. The three strong branches are combination of the bulk states and surface states, while the other three branches are mainly surface states. The two concentric surface FSs at BZ center are not distinguishable by 24 eV photons.